



Holocene Tsunamis in Avachinsky Bay, Kamchatka, Russia

TATIANA K. PINEGINA,¹  LILYA I. BAZANOVA,¹ EGOR A. ZELENIN,² JOANNE BOURGEOIS,³ ANDREY I. KOZHURIN,^{1,2}
IGOR P. MEDVEDEV,⁴ and DANIL S. VYDRIN⁵

Abstract—This article presents results of the study of tsunami deposits on the Avachinsky Bay coast, Kurile-Kamchatka island arc, NW Pacific. We used tephrochronology to assign ages to the tsunami deposits, to correlate them between excavations, and to restore paleo-shoreline positions. In addition to using established regional marker tephra, we establish a detailed tephrochronology for more local tephra from Avachinsky volcano. For the first time in this area, proximal to Kamchatka's primary population, we reconstruct the vertical runup and horizontal inundation for 33 tsunamis recorded over the past ~ 4200 years, 5 of which are historical events – 1737, 1792, 1841, 1923 (Feb) and 1952. The runup heights for all 33 tsunamis range from 1.9 to 5.7 m, and inundation distances from 40 to 460 m. The average recurrence for historical events is ~ 56 years and for the entire study period ~ 133 years. The obtained data makes it possible to calculate frequencies of tsunamis by size, using reconstructed runup and inundation, which is crucial for tsunami hazard assessment and long-term tsunami forecasting. Considering all available data on the distribution of historical and paleo-tsunami heights along eastern Kamchatka, we conclude that the southern part of the Kamchatka subduction zone generates stronger tsunamis than its northern part. The observed differences could be associated with variations in the relative velocity and/or coupling between the downgoing Pacific Plate and Kamchatka.

Key words: Kamchatka, subduction zone, Avachinsky Bay, Earthquake, tsunami deposits, tephrochronology, paleo-shoreline reconstruction, Avachinsky volcano.

Electronic supplementary material The online version of this article (<https://doi.org/10.1007/s00024-018-1830-0>) contains supplementary material, which is available to authorized users.

¹ Institute of Volcanology and Seismology FED RAS, 9 Piip Boulevard, Petropavlovsk-Kamchatsky 683006, Russia. E-mail: pinegk@yandex.ru

² Geological Institute RAS, 7 Pyzhevsky Lane, Moscow, Russia.

³ Earth and Space Sciences, University of Washington, Seattle, USA.

⁴ P.P. Shirshov Institute of Oceanology RAS, 36 Nakhimovskiy Prospekt, Moscow, Russia.

⁵ Lomonosov Moscow State University, 1 Leninskie Gory, Moscow, Russia.

1. Introduction

For most coastal countries, historical tsunami records are quite short and are reliable only for the last several centuries. However, for establishing tsunami recurrence and intensity and for developing tsunami hazard zoning, a much longer catalog of tsunami data is required because catastrophic tsunamis occur infrequently, on a time scale of hundreds to a few thousand years (Bourgeois 2009). A reliable prediction of possible tsunami parameters at specific parts of the coast cannot rely on data from one or a few historical events.

At present, many scientists are studying prehistoric-tsunami (paleotsunami) deposits to restore the parameters of ancient tsunamis over thousands of years. Research groups have applied this approach since the 1990s, and it became widely used after the disastrous 2004 Indian Ocean tsunami. Methods applied, as in this paper, can produce detailed geological records of tsunamis back to about 6000 years ago, following the rapid early-to-middle Holocene rise in sea level (Woodroff and Horton 2005). Preservation of this record also depends on the presence of accumulative coastal settings and on the coastal tectonic regime.

In Russia, the Far Eastern (Pacific) coast is the most affected by tsunamis (Soloviev and Ferchev 1961; Soloviev 1972, 1978). The most dangerous tsunamigenic earthquakes in the Russian Far East occur along the Kurile-Kamchatka subduction zone, along the northwestern margin of the Pacific Ocean. The catalog of historical tsunamis for this region is short (first event 1737) and quite incomplete before the twentieth century (Zayakin and Luchinina 1987; Pinegina and Bazanova 2016). Even recent tsunamis (e.g., 1997 Kronotsky) have geographically limited

data (Bourgeois and Pinegina 2018). Therefore, studies of tsunami deposits are a key source of reliable information about these hazardous events.

In this paper, we present new, detailed information about tsunami deposits for the past ~ 4200 years on the Avachinsky Bay coast, Kamchatka Peninsula (Fig. 1). To determine paleotsunami runups and inundations for different time intervals we apply corrections for vertical movement of the coast and for horizontal seaward progradation.

On most coasts along eastern Kamchatka, Holocene marine accumulative (wave-built) terraces as expressed in modern topography are typically not older than ~ 2000 years (Pinegina 2014), limiting paleotsunami data and analysis. However, partly because of intense search and study, we have established a > 4000 -year record in the case herein. This study thus maximizes extension of the tsunami catalog for Kamchatka. This task is particularly important because the central coast of Avachinsky Bay (named Khalaktyrsky beach) is the recreational zone of Petropavlovsk-Kamchatsky city and adjacent

settlements, and includes industrial facilities and agricultural land.

Avachinsky Bay is located on the southeast coast of Kamchatka Peninsula (Fig. 1). Petropavlovsk-Kamchatsky, the most populated city and the regional center (Fig. 2), is situated in its middle part, on the northern bank of Avachinsky Harbor.

2. Review: Seismic and Volcanic Activity in the Avachinsky Bay Region from Historical Records and Previous Studies

2.1. Tsunamigenic Earthquakes

By the beginning of the twentieth century, a world network of seismic stations was already capable of recording earthquakes of magnitude $M \geq 7.0$ from the Kamchatka region. The first seismic station in Kamchatka (in Petropavlovsk-Kamchatsky) was established in 1915. Since then two great earthquakes (04 Feb 1923 and 05 Nov 1952) along the Kamchatka subduction zone generated tsunamis that affected Avachinsky Bay (Fig. 1). Another large earthquake, on 05 Nov 1959 (Fig. 1) occurred at greater depth and caused a small tsunami of up to 2 m on the northern coast of Avachinsky Bay (Zayakin and Luchinina 1987; Gusev 2004). The 1960 Chilean tsunami did not exceed the active beach along Avachinsky Bay.

In 1959, the seismic station “Petropavlovsk” became involved in a tsunami warning system. The period of detailed seismological observation in Kamchatka and the Kurile Islands began in 1961. Since then, there have been several strong earthquakes accompanied by a tsunami: Ozernovskoe 1969, Kronotskoe 1997, and Central-Kuriles 2006 and 2007. However, on the coast of Avachinsky Bay, there were no noticeable tsunamis observed during this period—they were recorded only by the tide gauge in Petropavlovsk-Kamchatsky, and their amplitude did not exceed few cm. The information about parameters of significant historical tsunamis along Avachinsky Bay has been refined and significantly supplemented during the study of their deposits (Pinegina and Bazanova 2016; this study; Fig. 3).

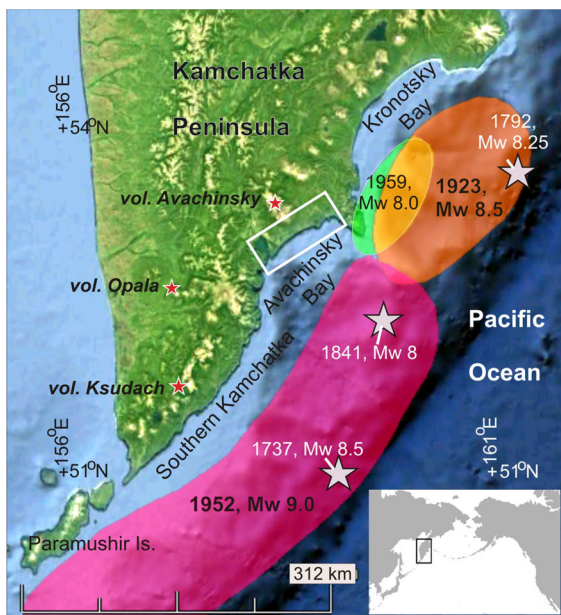


Figure 1

Location of local historical tsunamigenic earthquakes affecting the Avachinsky Bay coast (modified from Gusev 2004, 2006). Rupture areas for twentieth century earthquakes; pre-twentieth century earthquakes show estimated epicenters. See Fig. 2 for general map and features of Kamchatka. The white rectangle shows the position of Fig. 3

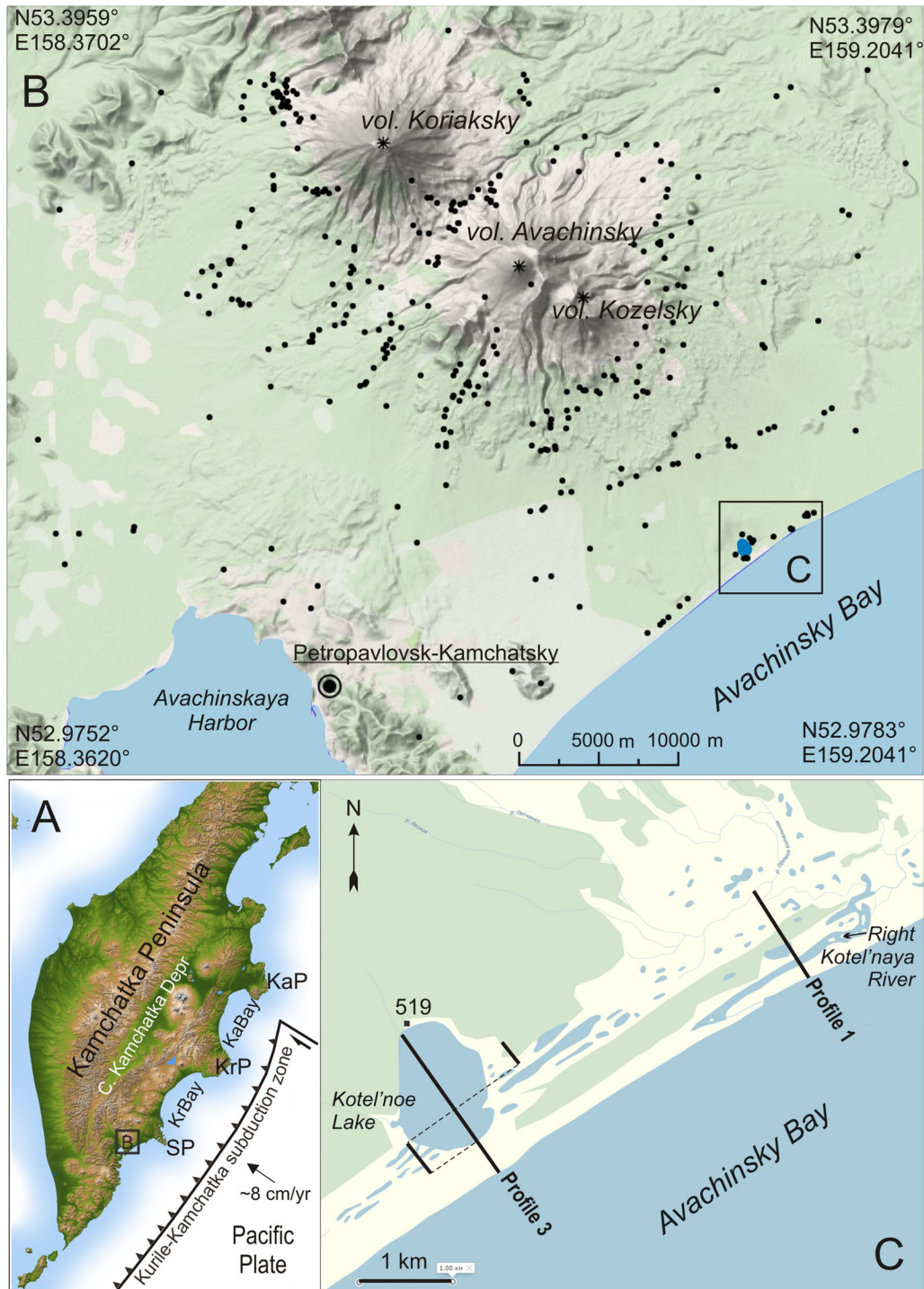


Figure 2

Field research area and setting: **a** General map of Kamchatka Peninsula with location of the field area (black box, **b**); sub-peninsulas and bays: *SP* Shipunsky Peninsula, *KrP* KrBay—Kronotsky Peninsula and Bay, *KaP* KaBay—Kamchatsky Peninsula and Bay; also Central Kamchatka Depression. **b** Observation points (black dots) in the vicinity of Avachinsky volcano where the geological sections of Holocene soil and peat were studied and sampled for tephrostratigraphy; **c** the site of detailed studies on the coast of Avachinsky Bay, locating profiles 1 and 3 and key peat section #519. Additional measurements and excavation descriptions were made along parallel profiles near profile 3, on either side of Kotel'noe Lake

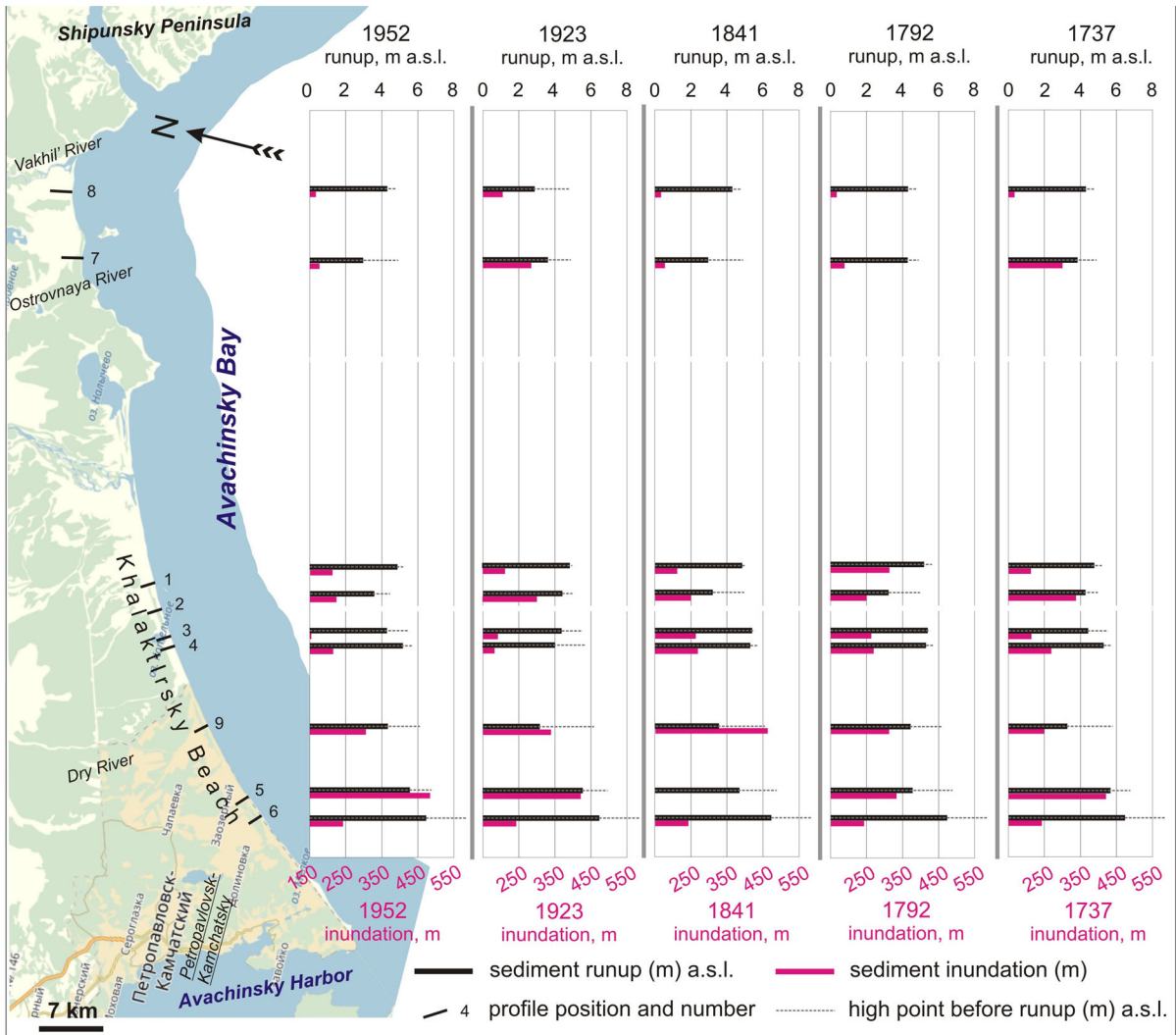


Figure 3

Tsunami-sediment runup, inundation, and high point before runup for historical tsunamis on the Avachinsky Bay coast (data in Pinegina and Bazanova 2016 with additional data from 2016 to 2017 field studies). Inundation axes start from 150 m for clarity of comparison between the events. The topographic map was downloaded from the cartographic web service Yandex Maps (<https://yandex.ru/maps/>). Modern coastal topography is used for these historical events; eighteenth century shoreline may have been 50 ± 25 m narrower

2.2. Tsunamis and Tsunami Deposits

A catalogue of historical tsunamis affecting the Kamchatka coast was compiled by Zayakin and Luchinina (1987), including pre-twentieth century tsunamigenic earthquakes in 1841, 1792 and 1737 (Figs. 1, 3). Strong Kuril-Kamchatka tsunamis have also been recorded all around the Pacific (NCEI database: <https://www.ngdc.noaa.gov/hazard/hazards.shtml>). The NCEI database indicates that Kamchatka

tsunamigenic earthquakes with $M_w \geq 8.3$ have caused dangerous transoceanic tsunamis. Due to geographical location, tsunamis from Kamchatka most strongly affect the Hawaiian Islands (see Table S1 in the Electronic Supplement). Far-field tsunami records supplement the limited Kamchatka data in the period of macroseismic observations.

The first investigation of tsunami deposits along the Avachinsky Bay coast was conducted in summer

2000. At that time, we described the deposits of 13 tsunamis in the last ~ 3500 years (Pinegina et al. 2002). At the time of this work the region's tephrostratigraphy was not studied in sufficient detail, so the age of some historical tsunamis was determined incorrectly. The paleotsunami history was also incomplete, and runup and inundation were presented without reconstructing the ancient shorelines. Newly updated data on historical tsunamis is presented in Pinegina and Bazanova (2016), and a review of Kamchatka paleotsunamis for the past 1500–2000 years is presented in Pinegina (2014).

2.3. Ashfalls

For stratigraphic markers in this study area, an area which we call “Kotel’ny”, we have used three well-known tephra from large Holocene eruptions on southern Kamchatka (Braitseva et al. 1997a, b; Melekestsev et al. 1996) as well as additional, more local tephra from Avachinsky volcano. The geological sections in our field site include regional marker ashes from Ksudach volcano (KSht₃—AD 1907, KS₁—1800 ¹⁴C BP) and Barany Amphitheatre crater, formed at the foot of Opala volcano (OP—1500 ¹⁴C BP) (Fig. 1, Table S4). The field site, moreover, is located 22–23 km southeast of the active crater of Avachinsky volcano (Fig. 2), whose Holocene tephra have been repeatedly dispersed in the region.

The eruptive history of Avachinsky volcano for the past 12,000 years has been reconstructed by detailed geologic, stratigraphic and tephrochronological studies (Braitseva et al. 1998; Bazanova 2013). The list of known Avachinsky eruptions includes 156 events, recorded as deposits of ashfalls and pyroclastic flows, of which 118 tephra layers belong to the active Young Cone. Individual layers have been traced in sections along radial and circular profiles around the crater (Fig. 2b), with tephra identification confirmed by mineralogical and chemical analyses. Radiocarbon dating helped verify tephra correlations: 189 radiocarbon dates were used for stratigraphic and chronological reconstructions (Bazanova 2013 and earlier), of which 54 are reported herein (Table 1; Fig. 4). Isopach maps have been compiled for most Avachinsky fall units, and as a result its dispersal axes and areas have been determined (Bazanova et al. 2001, 2003, 2005).

In this study, at the Kotel’ny site, we take advantage of the long record of tephra from Avachinsky volcano in its several stages of eruptive history. The oldest parts of our sections generally include thin layers from the marginal zones of ashfall tephra associated with the so-called Andesite-stage eruptions (7250 – 3500 ¹⁴C BP) (Braitseva et al. 1998). Juvenile rocks of this Andesite stage are mostly low-K andesite (white, yellow, light gray pumice, sometimes with dense gray fragments). Toward the end of the Andesite stage, two initial catastrophic eruptions of the active Young Cone of Avachinsky volcano occurred about 3500 and 3300 ¹⁴C years BP and produced widespread fallout deposits (Bazanova et al. 2003), including at the Kotel’ny site.

Over the past 3800 years, the SSE oceanward sector of the volcano has remained one of the areas most exposed to ashfalls (Bazanova et al. 2001). Tephra units of the Young Cone are predominantly composed of juvenile black or dark gray and brown scoria of low- to medium-K basaltic andesite (Bazanova et al. 2003; Krashennikov et al. 2010), some with rare small lapilli of andesitic pumice. In historical time, Avachinsky ashfalls occurred at the Kotel’ny site in 1779, 1827, 1855 and 1945. The characteristics of these eruptions and the peculiarities of their tephra distribution on the coast of Avachinsky Bay have been considered in earlier publications (Melekestsev et al. 1994a, b; Pinegina and Bazanova 2016).

We have adopted a new system for indexing the eruptions of the Avachinsky volcano (as in Pinegina and Bazanova 2016). Early tephrochronological studies considered five paroxysmal eruptions and assigned them codes AV₁–AV₅ (Braitseva et al. 1997a, b). Later publications (Braitseva et al. 1998; Bazanova et al. 2003) proposed indexing style IAV_x for the Andesite-stage eruptions and IIAV_x for the Young Cone stage, where the codes include the stage number and the sequence number (*x*) of the explosion (see Table S2). However, further work has enumerated about 150 eruptive events (this paper; Bazanova 2013) and revealed the flaws of using such indexing, which makes tephra identification, section description, text review and scientific discussion difficult, even for the authors. Therefore, for prehistoric eruptions of Avachinsky volcano, we index the

Table 1
Radiocarbon dates and ages of Avachinsky volcano eruptions

S/ N	Tephra code ^a	Laboratory number ^{b, c}	¹⁴ C age (years before 1950 AD)	Average ¹⁴ C age ^d	Calibrated age AD/BC (probability 95.4%) ^d	Material for dating	Place of sampling
1	AV550	GIN-11369 (C) GIN-11370	540 ± 60 570 ± 70	553 ± 46	AD 1299(1371)1440	Peat above the tephra Peat under the tephra	Kotel'noe Lake, the Pacific coast Kotel'noe Lake, the Pacific coast
2	AV580	GIN-11370 (C) GIN-7804	570 ± 70 580 ± 60	576 ± 46	AD 1296(1353)1427	Peat above the tephra Peat under the tephra	Kotel'noe Lake, the Pacific coast Kotel'noe Lake, the Pacific coast
3	AV750	GIN-8105 (H ₁) GIN-7803	740 ± 110 730 ± 50	732 ± 46	AD 1210(1272)1388	Soil above the tephra Peat under the tephra	Koriaksky volcano Kotel'noe Lake, the Pacific coast
4	AV800	GIN-7802 (H')	800 ± 40		AD 1166(1233)1278	Peat under the tephra	Kotel'noe Lake, the Pacific coast
5	AV1000	GIN-13163 (C) GIN-7801 (H')	1020 ± 60 1000 ± 40 1000 ± 40 1020 ± 70	1006 ± 25	AD 985(1020)1147	Peat above the tephra Peat above the tephra Peat under the tephra Peat under the tephra	Zhupanov ridge, Shaibnaya River Kotel'noe Lake, the Pacific coast Kotel'noe Lake, the Pacific coast Zhupanov ridge, Shaibnaya River
6	AV1100	GIN-7800 (H')	1000 ± 40 1160 ± 40	1081 ± 29	AD 894(965)1018	Peat above the tephra Peat under the tephra	Kotel'noe Lake, the Pacific coast Kotel'noe Lake, the Pacific coast
7	AV1250	GIN-7798 (H')	1250 ± 60 1260 ± 40	1257 ± 34	AD 670(738)868	Peat above the tephra Soil under the lahar deposit	Kotel'noe Lake, the Pacific coast Avachinsky volcano
8	AV1600 ^f	GIN-6934 (C) IVAN-399 (H ₁) IVAN-593 (C) GIN-7796 (H')	1620 ± 80 1570 ± 110 1640 ± 60	1622 ± 45 1623 ± 44	AD 264(424)541 AD 335(437)545	Peat above the tephra Peat under the tephra Peat under the tephra	Petropavlovsk-Kamchatsky Hot River, Nalichevo Valley Kotel'noe Lake, the Pacific coast
9	AV2000	GIN-11375 (H ₁) GIN-11376 (C)	1960 ± 40 2010 ± 60	1975 ± 34	BC 48(AD26)AD115	Peat above the tephra Peat under the tephra	Kotel'noe Lake, the Pacific coast Kotel'noe Lake, the Pacific coast

Table 1 continued

S/ N	Tephra code ^a	Laboratory number ^{b,c}	¹⁴ C age (years before 1950 AD)	Average ¹⁴ C age ^d	Calibrated age AD/BC (probability 95.4%) ^d	Material for dating	Place of sampling
10	AV2400	GIN-11378 (H ₁) GIN-8516 (H ₁)	2380 ± 40 2400 ± 50	2388 ± 32	BC 729(464)396	Peat under the tephra Peat under the tephra	Kotel'noe Lake, the Pacific coast Left Avacha River
11	AV2450	GIN-11379 (H ₁)	2460 ± 40		BC 761(603)415	Peat under the tephra	Kotel'noe Lake, the Pacific coast
12	AV2550	GIN-6931 (H ₁) GIN-11381 (C)	2580 ± 60 2550 ± 40	2559 ± 34	BC 806(764)549	Soil above the tephra Peat under the tephra	Avachinsky volcano Kotel'noe Lake, the Pacific coast
13	AV2650	GIN-10639 (C) GIN-6909 (C + H ₁)	2650 ± 70 2670 ± 60	2662 ± 46	BC 912(830)787	Tephra-containing peat Tephra-containing soil	Vakhil' River Avachinsky volcano
14	AV2700	GIN-7439 (C + H ₁) IVAN-562 GIN-11382 (H ₁)	2720 ± 70 2710 ± 70 2710 ± 30	2711 ± 26	BC 906(858)811	Soil above the tephra Charcoal from PFI ^e deposits Peat under the tephra	Avachinsky volcano Avachinsky volcano Kotel'noe Lake, the Pacific coast
15	AV2800	GIN-11383 (H ₁)	2790 ± 30		BC 1011(941)846	Peat under the tephra	Kotel'noe Lake, the Pacific coast
16	AV3100	GIN-11385 (C)	3100 ± 40		BC 1449(1354)1260	Peat under the tephra	Kotel'noe Lake, the Pacific coast
17	AV3300 ^f	GIN-6929 (C) GIN-6896 GIN-6897 GIN-11374 (H ₁)	3300 ± 80 3270 ± 40 3280 ± 40 3260 ± 70	3279 ± 28 3276 ± 25	BC 1678(1523)1463 BC 1617(1558)1501	Soil above the tephra Charcoal from PFI deposits Charcoal from PFI deposits Peat under the tephra	Avachinsky volcano Avachinsky volcano Avachinsky volcano Kotel'noe Lake, the Pacific coast

Table 1 continued

S/ N	Tephra code ^a	Laboratory number ^{b,c}	¹⁴ C age (years before 1950 AD)	Average ¹⁴ C age ^d	Calibrated age AD/BC (probability 95.4%) ^d	Material for dating	Place of sampling
18	AV3500 ^e	IVAN-708 (C)	3440 ± 50	3510 ± 17	BC 1885(1877, 1840, 1827, 1795, 1782) 1745	Peat above the tephra	Sharomy vil., Kamchatka R.
		IVAN-294 (C)	3470 ± 120	3508 ± 16	BC 1891(1824)1767	Soil above the tephra	Uzon caldera
		GIN-7129 (C)	3450 ± 40			Wood buried by PFI deposits	Avachinsky volcano
		GIN-7128 (C)	3510 ± 100			Wood buried by PFI deposits	Avachinsky volcano
		GIN-7134	3570 ± 40			Charcoal from PFI deposits	Avachinsky volcano
		IVAN-815	3580 ± 70			Charcoal from PFI deposits	Avachinsky volcano
		GIN-6056	3560 ± 50			Soil under PFI deposits	Avachinsky volcano
		GIN-7130 (C)	3580 ± 90			Soil under the tephra	Avachinsky volcano
		GIN-6361 (C)	3570 ± 60			Soil under the tephra	Avachinsky volcano
		IVAN-843 (C + H ₁)	3470 ± 70			Peat under the tephra	Kamchatka R., the Big Yar
		IVAN-385 (H ₁)					Kotel'noe Lake, the Pacific coast
		GIN-11372 (C)					
19	AV3700	GIN-11371 (C)	3680 ± 70	3685 ± 68	BC 2284(2076)1892	Peat under the tephra	Kotel'noe Lake, the Pacific coast
		GIN-6917 (C)	3750 ± 250			Soil under the tephra	Avachinsky volcano
20	AV3800	GIN-6917 (C)	3750 ± 250	3811 ± 24	BC 2339(2247)2146	Soil above the tephra	Avachinsky volcano
		IVAN-561	3760 ± 60			Charcoal from PFI deposits	Avachinsky volcano
		IVAN-844 (C + H ₁)	3750 ± 120			Soil under the tephra	Avachinsky volcano
		GIN-7440 (C + H ₁)	3800 ± 100			Soil under the tephra	Avachinsky volcano
		Le-7866	3820 ± 30			Peat under the tephra	Zhupanovsky volcano, SE foot
		GIN-6916	3860 ± 70			Soil under the tephra	Avachinsky volcano

^aCodes of Avachinsky volcano tephra include index AV and rounded average radiocarbon age (up to 50 years or up to 10 years for the intervals with a higher frequency of eruptions); for codes in previous publications see Table S2

^bRadiocarbon dating from the bulk samples was carried out at the Geological Institute of the Russian Academy of Sciences, Moscow (GIN) and the Institute of Volcanology, Far-Eastern Branch of the Russian Academy of Sciences, Petropavlovsk-Kamchatsky (IVAN), and the Institute for the History of Material Culture of the Russian Academy of Sciences, Saint-Petersburg (Le)

^cAlkaline extracts: C—cold (first); H₁—hot (second); H₂—hot (the third); H₃—hot (in the case when only a hot extracts were used)

^dAverage radiocarbon and calibrated ages of tephra calculated with program OxCal v.4.24 (Bronk 2009) with the IntCal13 calibration curve (Reimer et al. 2013)

^ePFI—pyroclastic flow

Bold italics—data published in: ^f(Dirksen and Bazanova 2010); ^g(Bazanava et al. 2003, 2016)

3. Methods

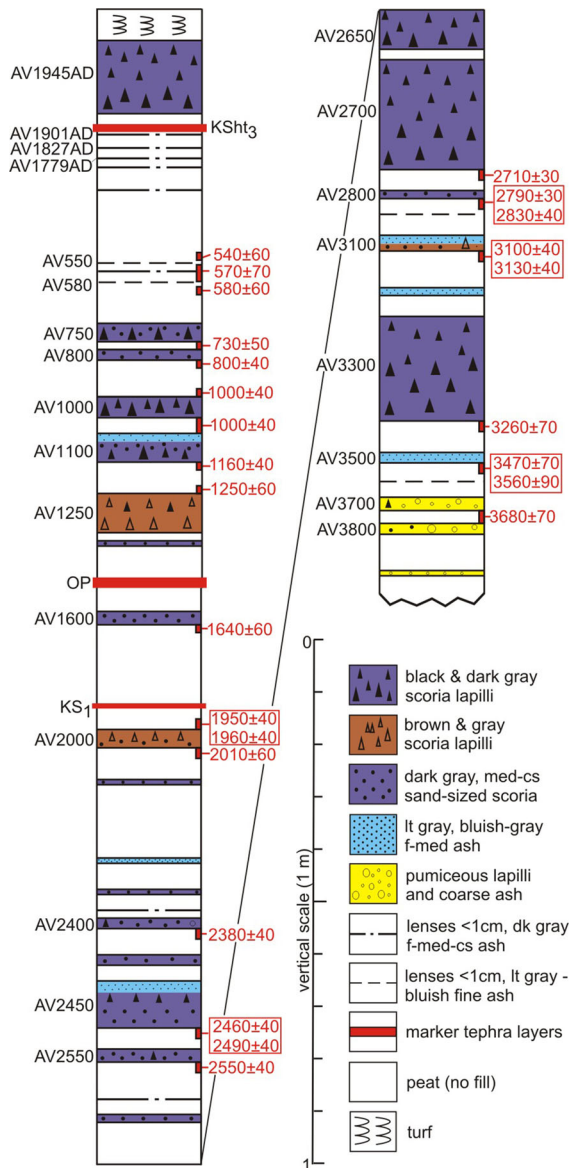


Figure 4

Key peat section near Kotel'noe Lake (site 519). Location of the section is shown in Fig. 2c and Fig. S2. Codes and ages of tephra layers as in Tables 1 and 2, and Tables S3 and S4. Radiocarbon dates are in red; dates on successive alkaline extractions from the same sample are shown in boxes (see Table 1)

tephra layers by volcano (AV) and a rounded ^{14}C age, which makes the tephra stratigraphy clearer. We summarize the new and old eruption codes in Table S2 to support comparison of this article to previous publications with different codes for the same eruptions.

To start, we interpreted satellite imagery to identify the oldest beach ridges preserved along the present coast of Avachinsky Bay. We used aerial imagery and declassified KH-9 Hexagon stereoscopic imagery (scanned films provided by the US Geological Survey) and imagery from cartographic web services (Google Earth, Yandex Maps, Bing Maps), where available, with resolution of $\sim 4\text{--}6$ m per pixel. We considered profiles 1 and 3, across the broadest accumulative marine terraces, as most promising for our studies because they preserve the oldest coastal accumulations (Fig. 2a, Fig. S1, Fig. S2). Older, lower beach ridges that have been partially buried by peat can be identified as linearly elongated vegetation “islands” clearly visible on multispectral images, even if they do not differ in height from the surrounding surface. The possibility to make excavations and coring operations in the wetlands depends on site accessibility and the level of groundwater, the latter elucidated by spectral signatures corresponding to different vegetation types. At times we used a pump to access levels under the water table. Outcrops along streamcuts through beach ridges are also a significant source of information, particularly where the channel is orthogonal to a beach ridge.

We measured nine topographic profiles perpendicular to the shoreline along ~ 70 km of Avachinsky Bay coastline (Fig. 3) using a Trimble M-3 total station with distance measurement accuracy of ± 3 mm/km and angular accuracy of $\pm 1''$. The heights of all the points measured along profiles were corrected according to known heights from the Reference State Geodetic Network. The lengths of profiles 1 and 3 are about 1100 and 1500 m, respectively; profile 3 is a composite to include the area submerged by Kotel'noe Lake (Fig. 2c). The height of beach ridges along the profiles ranges from 3 to 5.5–6 m above sea level (a.s.l.). The width of the active beach in this area is about 70 m, with its upper limit (where vegetation becomes dense) at elevations of 4.5–5.0 m. The shape of the profiles is saw-toothed with a slight increase in elevation of the beach ridges towards the sea. Such a shape indicates a net relative-

Table 2

continued

Tsunami	2.9	425 ± 60	4.3	4.2	90 ± 90	5.3	17	21	30
AV3500									
Tsunami	3.2	196 ± 60	4.3 ^e				18		31
	2.4	565 ± 60							
AV3700									
Tsunami				4.3	40 ± 40	4.7		22	32
AV3800									
Tsunami	2.8	365 ± 15	4.3				19		33

The left column contains only dated units of tephra. The dark gray fill of a cell means the presence of tephra in the excavations along the profile, light gray indicates the presence of tephra traces; unshaded implies the absence of tephra

^a*H*, sediment runup elevation (m above sea level, corrected for paleotsunami cases)

^b*L*, sediment inundation limit (m from the shoreline, corrected for paleotsunami)

^c*h*, maximum profile elevation between the shoreline and sediment inundation limit (m above sea level, corrected for paleotsunami)

^dPublished in Pinegina and Bazanova (2016)

^eTsunami deposits from river outcrop sections; the tsunami probably propagated up the Right Kotel'naya River

sea-level rise of no more than a few meters from the Late-Middle Holocene to the present.

Along profiles 1 and 3 we made 37 excavations to a depth of ~ 1 to ~ 3.5 m and described tephra layers and tsunami deposits (Figs. S1, S2). Excavations were made on or between almost every beach ridge; distances between excavations vary from 10–20 to 50–70 m. The depth of the pits depended on the thickness of soil mantling the relict (not active at present) beach ridges. Usually, we dug to a depth of 1–1.5 m below the soil-pyroclastic sequences into clean sand, which represents the ancient active beach. The upper age boundary of the time when a given beach ridge was no longer active is determined by the age of the oldest tephra at the base of the soil (as in Pinegina et al. 2013). Ages of tsunami deposits are bracketed by the ages of underlying and overlying tephra.

Peat sections (e.g., Fig. 4; Fig. S2) were studied in detail because peat's high rate of accumulation permits good preservation of even thin tephra and tsunami deposits. Moreover, peat can be used for radiocarbon dating. We cored the peat up to a depth of 4–5 m with a manual peat corer, and then the cores were described and sampled in detail.

3.1. Tephrochronology

Tephrochronological studies with radiocarbon dating provide comprehensive stratigraphic and chronological control for prehistoric events. This method has been successfully applied in Kamchatka, for example to determine the ages of landforms and of event deposits (many references). A primary goal of the Kotel'ny site study was to find and study a reference section with the maximum number of tephra layers. We succeeded in generating such a section from the peat bog on the NW side of Kotel'noe Lake (Site 519, Figs. 2c, 4).

The tephrostratigraphic framework in this reference section, where Avachinsky tephra layers predominate, goes back ~ 4200 years (i.e., the calibrated age BP of AV3800). The tephra layers were described by stratigraphic position and by appearance—thickness, grain size, grading and color of particles, lithic content, textural features, etc. They were identified/indexed by tracking and comparison with previously studied tephra in sections toward Kozelsky volcano (Fig. 2b). We collected peat samples for radiocarbon dating (Fig. 4), which we used for chronological reconstructions.

With this reference section, we made a layer-by-layer study of Holocene soil-pyroclastic sequences, including tsunami deposits, in coastal excavations along profiles 1 and 3 (Figs. S1, S2). The known and dated tephra horizons correlated from our reference section allowed us to trace tsunami deposits along and across beach ridges for mapping and for age estimation of each tsunami horizon.

3.2. Tsunami Deposits

In each excavation along a measured profile, we identified tsunami deposits, and described their thickness, grain size, stratification and grading; we took selected samples and photo-documented the section walls. Tsunami deposits in soil-pyroclastic sequences at the Kotel'ny site are generally thin sand layers (up to 20 cm), which tend to decrease landward in both layer thickness and grain size. The deposits consist mostly of the same material as the marine wave-built terrace and active beach—mainly dark, medium—to coarse-grained sand with some layers and patches of rounded gravel and pebbles. Once deposited, the tsunami layers are protected from erosion by dense coastal vegetation and are buried in the soil-pyroclastic sequence. If a tsunami leaves a deposit when there is snow cover on the coast, then as the snow melts, the deposit is lowered to the turf

surface, where the deposit is protected from erosion by old and new vegetation (MacInnes et al. 2009a; Bourgeois and Pinegina 2018). We used standard criteria for tsunami-deposit identification along the Kuril-Kamchatka coastline, as described in previous papers (e.g., Pinegina et al. 2000; Bourgeois et al. 2006; Pinegina 2014). Here we will not describe these criteria in detail; we only note that the study sites are away from eolian, fluvial and storm influence.

It is possible to evaluate a minimum distance (sediment inundation, L) and a minimum height (sediment runup at inundation point, H) of past historical and prehistoric tsunamis from tsunami-deposit distribution (Fig. S3; also Bourgeois and Pinegina 2018). The most landward section with a given tsunami deposit approximates tsunami runup and inundation, limited by distance to the next landward section and also by the assumption that the tsunami transported sediment to its landward limit. To verify a pinch-out line, we try to control for non-preservation by examining more than one more section landward. The pinch-out elevation for a given tsunami deposit on a particular profile specifies a minimum wave height. If the tsunami crossed the beach-ridge plain orthogonally, the reconstructed tsunami height may also be bounded by the maximum elevation (h) of beach ridges between the

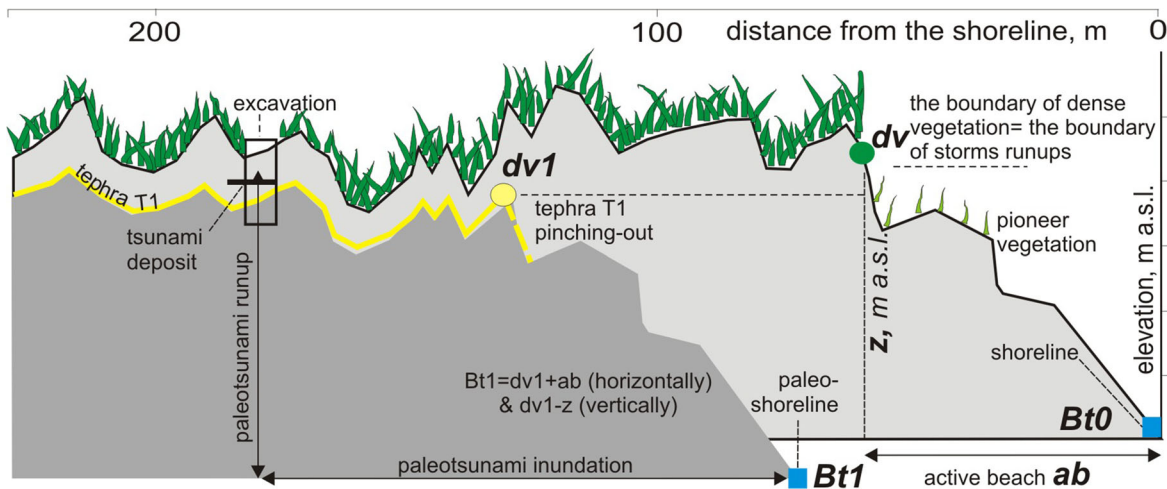


Figure 5

Reconstruction of a paleo-shoreline position (example of a fragment of profile 3 with a schematic tephra T1): dv beginning of dense vegetation (present day upper boundary of the active beach); $dv1$ upper boundary of the active beach at the time of T1 tephra fall; z elevation (m a.s.l.) of dv ; ab distance between dv and modern shoreline $Bt0$ (blue square); $Bt1$ shoreline at the time of T1 tephra fall

shoreline and tsunami-deposit pinch-out (Fig. S3). Tsunami heights closer to the shoreline on a relatively flat plain will be higher than runup H in any case, to drive the tsunami to its landward limit L (Fig. S3).

Our calculation of tsunami runup and inundation may be somewhat underestimated because the tsunami flow can go farther landward than its sediments. Some recent tsunami studies have shown that actual (water) runup did not much exceed sediment runup in several cases (MacInnes et al. 2009a, b). However, studies of 2011 Tohoku tsunami deposits show that in some cases the difference between water runup and sediment runup can be significant (Goto et al. 2011; Abe et al. 2012).

3.3. Estimation of Paleotsunami Size by Reconstructing Ancient Shoreline Position

For accurate estimation of paleotsunami runup and inundation, it is necessary to reconstruct the paleoshoreline position at the time of tsunami propagation as well as subsequent changes in surface elevation. We use tephra stratigraphy and tephra mapping along measured topographic profiles to reconstruct paleoprofiles and paleoshoreline positions (as in Pinegina et al. 2013; Pinegina 2014; MacInnes et al. 2016).

Volcanic ash-falls accumulate and are preserved on a vegetated (marine-terrace) surface, but at the active beach, tephra will be washed away during the next storm. In a prehistoric case, the same holds true, so the landward limit of the active beach at the time of the ash-fall is the modern tephra pinch-out line (Fig. 5). For further calculations, we need to assume that storm conditions at a particular point (profile) on the coast have remained about the same, so a vertical shift from pinch-out line (e.g., dv_1 on Fig. 5) to the modern active beach limit (dv) is due primarily to vertical tectonic movement or to eustatic sea-level change; the latter is minimal during the Late Holocene.

The calculation of the paleoposition relative to the modern shoreline ($x; y = 0; 0$) (Bt0 on Fig. 5) of any point on a profile at the time of a particular tephra fall comprises two steps. First, subtract the

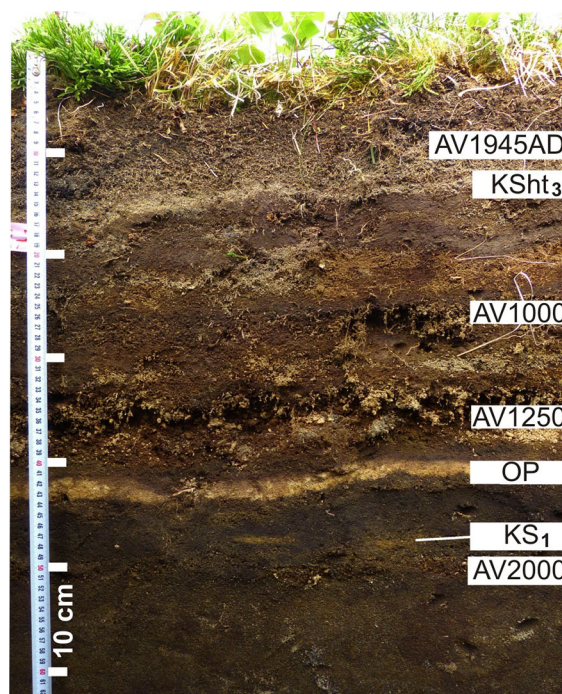
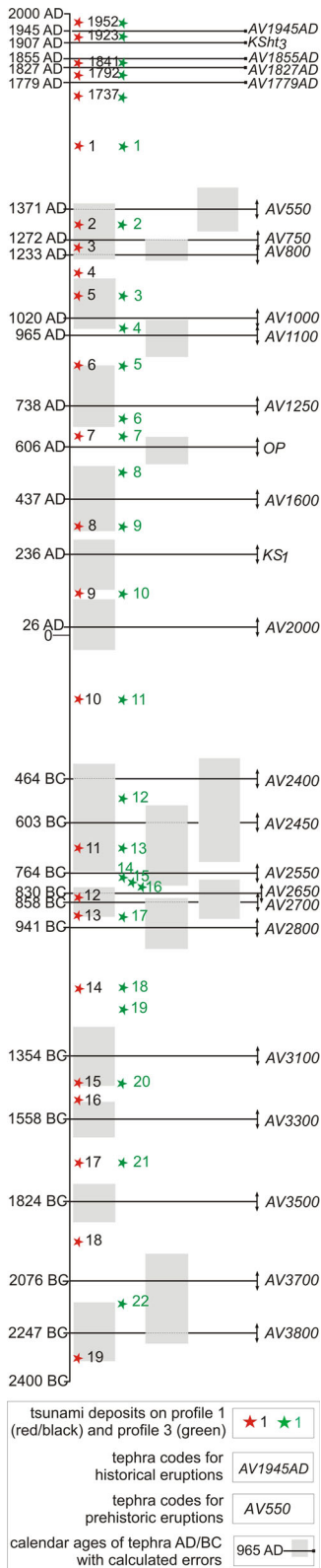


Figure 6
Section 727 (Figure S2, profile 3), where the regional marker tephra (KSht₃, OP, KS₁) are distinguished and easily recognized due to their bright color and individual features (Table S4). Also labeled are some of the most clearly visible (on this photo) horizons of Avachinsky tephra

($x; y$) coordinates of tephra base at its pinch-out (dv_1 on Fig. 5) from the ($x; y$) coordinates of the tephra base at a given excavation point (excavation in Fig. 5). Second, add the width of the modern active beach and the height (a.s.l.) of its upper boundary (dv on Fig. 5) to the coordinates calculated in the first step. If the point of pinch-out for a specific tephra (e.g., dv_1 for tephra T1) was not exposed in an excavation, we would place this point on the profile between the seawardmost T1-containing excavation and the next seaward excavation without T1. The error of such an estimation is roughly half the distance between the two excavations, which in this study did not exceed 60 m. We also correct for vertical displacement of paleoshorelines relative to modern sea level. That is, if the current elevation of the paleo- dv_1 point is below the present dv , we add the difference ($dv - dv_1$) between their elevations to the entire “old” (older than dv_1) part of the profile.



◀Figure 7

Composite chronological section from excavations along the Avachinsky Bay coast with positions of tephra and tsunami events. Tsunami are shown in the middle interval between two nearest tephra. Vertical axis indicates time in calendar years BC/AD. For tephra codes see Table 1 and Table S3. Tsunami numbers are same as in Table 2

4. Results and Discussion

During field surveys on the Avachinsky Bay coast, we excavated and described more than 100 geological sections on the Holocene accumulative marine terrace and on adjacent Late Pleistocene fluvioglacial and alluvial terraces (Fig. 2). Based on this work, we have created a tephrochronological framework, reconstructed the position of ancient shorelines, identified tsunami deposits and estimated tsunami recurrence rate and intensity.

4.1. Tephrochronology

We have obtained a reliable tephrochronological framework with radiocarbon dates for most of tephra horizons in our reference section, which has served as the basis for further stratigraphic and chronological comparisons. In the reference peat section (section 519, Fig. 2c) near Kotel'noe Lake, we identified 42 tephra layers from the past ~ 4200 years and generated radiocarbon dates for many of them (Fig. 4); some of these tephra, traced in other sectors of the volcano, were dated previously. Most (39) tephra are from Avachinsky volcano, including the four lowest, which belong to the final eruptions of the Andesite stage; the remaining 35 record activity of the Young Cone. We collected 26 ¹⁴C samples from key peat section 519 and obtained calibrated ¹⁴C ages (AD/BC) for most of the tephra (Fig. 4; Table 1, including prior dating). The even distribution of dates from the top of the peat section to the bottom, and the consistency of dates for each tephra unit, including dates from other sections (Table 1) support the reliability of the obtained dates. In addition to the reference peat section, we described 37 excavations and mapped tephra horizons along profiles 1 and 3 (Figs. S1, S2).

The strongest eruptions with a volume of pyroclastic material $\geq 0.1 \text{ km}^3$ are most clearly expressed

at the Kotel'ny site and are reliably recognized; these include: AV1945AD, AV750, AV1000, AV1100, AV1600, AV2650, AV2700, AV3300. These fall units have distinct dispersal axes directed to the SE (most), SSE, S, and E (Bazanova et al. 2005). It is also easy to identify the tephra of some moderate eruptions (AV1250, AV2450). However, some thin tephra layers in the 519 peat section are hardly visible or were unrecognized in the soil-pyroclastic sequences along profiles 1 and 3. For detailed descriptions of the individual horizons of tephra in these sections see Table S3.

In the field area, tephtras of the Avachinsky Young Cone stage are usually composed of black to brown scoria of various grain sizes, variable density, and almost uniform composition. The tephra from weak eruptions (e.g., AV550) or from the marginal ashfall zones of significant eruptions (e.g., AV3500) typically occur as thin layers or lenses of light gray and bluish-gray ash (Table S3).

Southern-Kamchatka-derived marker tephtras from Ksudach volcano and the Barany Amphitheatre crater are consistently present in both peat and soil-pyroclastic sequences (Figs. S1, S2). They are easily distinguished by their light color in otherwise dark-brown sections (Fig. 6). The characteristics of these tephtras are provided in Table S4.

4.2. Historical Tsunami Deposits on the Coast of Avachinsky Bay

Comparing available historical descriptions of tsunami heights on the Avachinsky Bay coast (Zayakin and Luchinina 1987) with sediment runups reconstructed in our studies, we conclude that they are roughly equal. The parameters for historical tsunamis on profiles 1–6 (Fig. 3) were determined earlier (Pinegina and Bazanova 2016); data for profiles 7–9 were obtained during fieldwork in 2016–2017 and are presented here for the first time. On the coast of Avachinsky Bay, we have identified deposits of five historical tsunamis (1737, 1792, 1841, 1923 and 1952). Their inundation did not exceed 480 m from the shoreline, with runup < 6.3 m a.s.l. (Fig. 3). On profiles 1 and 3, inundation of historical tsunamis did not exceed 310 m, with runup < 5.4 m a.s.l. (Table 2). The mean recurrence

rate of these strong (> 4–5 m runup) tsunamis over almost 300 years is one event per 55–56 years.

Analysis of these historical earthquakes and tsunamis (Figs. 1, 3) shows that tsunami sources at Avachinsky Bay can be located on the subduction zone within or north or south of the bay. That is, earthquakes with $M_w \sim 8$ –9 situated in south Kamchatka (e.g., 1952) and the southern part of Kronotsky Bay (e.g., 1923) may also generate dangerous tsunamis on the Avachinsky Bay coast.

4.3. Paleotsunami

Twenty-eight of the 33 tsunami deposits we have documented on profiles 1 and 3 are prehistoric (Table 2; Figs. S1, S2) and are shown as a composite section in Fig. 7. The oldest of these deposits lies just under the AV3800 tephra fall (~ 4250 calendar BP), and should be close to this age. Older tsunami deposits in the area are not preserved due to the absence of older marine terraces. We suppose that the main factors for this absence are the global Middle Holocene sea-level rise (Woodroff and Horton 2005) and an overall general net lowering of the central part of the Avachinsky Bay coast accomplished primarily by coseismic subsidence (Pinegina et al. 2015).

The runup heights for all tsunamis in profiles 1 and 3 (Table 2) vary from 1.9 to 5.7 m with a mean value of 4.1 m a.s.l. Tsunami inundation distances range from 40 to 460 m (most in ~ 150 –300 range), averaging 255 m, excluding tsunamis possibly propagated along the river (see Table 2 asterisk cases). The minimum highest point a tsunami had to exceed along a given topographic profile (h in Figure S3) ranges from 2.4 to 5.7 m with a mean of 5.15 m a.s.l. (Table 2).

From our data, we conclude that paleotsunami parameters for the past ~ 4.2 millennia are comparable to historical ones. However, horizontal inundation in prehistoric cases may be underestimated if it occurred before erosional shoreline retreat following coseismic subsidence. We think this underestimation is generally not important because on the Avachinsky Bay coast, we have been able to identify only three events of coseismic subsidence in the past ~ 4200 years (Pinegina et al. 2015), each event followed quickly by coastal progradation.

Because tsunami runup highly depends on coastal relief, we believe that horizontal inundation along lower, flatter profiles should be more informative for reconstructing tsunami intensity (strength, size). On steep slopes and cliffs close to the shoreline, the runup can be much greater, whereas on low-elevation, low-relief profiles, inundation will be greater. Moreover, even in the geographically limited case of our field area, the elevation of the coastal beach ridges in the southern part of the Khalaktirsky beach is slightly higher than on profiles 1 and 3. Respectively, the restored tsunami runups are also higher there (see Fig. 3). Thus, tsunami hazard analysis must take coastal topography into account, as well as both runup and inundation.

4.4. Analysis of Data Loss Depending on the Age of Tsunami Deposits

To evaluate the fidelity of long-term tsunami recurrence statistics, we need to estimate the quality of preservation of their deposits over a millennial time scale. This issue was considered in detail in a central Kuril Islands study (MacInnes et al. 2016). For our current study area, we tried to analyze tsunami-deposit preservation using various horizons of well-studied volcanic tephra as time benchmarks (Fig. 8).

A priori, we assume that the average recurrence interval of earthquakes and tsunamis on the millennial scale should be comparable for a given region because the seismic regime of the subduction zone varies on a longer time scale. Millennial intervals will

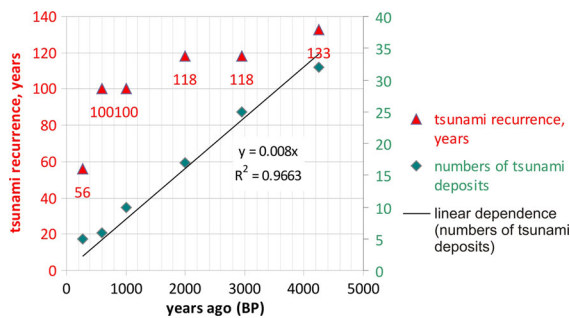


Figure 8

Analysis of tsunami deposit preservation and tsunami recurrence during the past ~ 4200 years along Avachinsky Bay. The time intervals are set by well-dated tephra

include seismic cycles of different events up to and including mega-earthquakes, such as AD 1952 and AD 1737 (Zayakin and Luchinina 1987). For our field site, the cumulative number of tsunami deposits for different time intervals (the past 4250, 2950, 2000, 1000, 600 and 279 years, based on calibrated tephra ages) is shown in Fig. 8. The cumulative number of deposits per time interval is well described by a linear relationship (R^2 close to 1). The average tsunami-deposit recurrence for the same time intervals (red numbers in Fig. 8) is more variable but for the last ~ 600, 1000, 2000 and 2950 years the average frequency of tsunamis was almost the same, at 1 event per 100–118 years. For the past 4250 years, the average tsunami-deposit frequency is reduced a little (1 event in 133 years), which could be due to poorer preservation, or to fewer sections studied. The shortest time interval (279 years, delimited by the 1737 tsunami deposit) includes only the historical period when tsunami deposits were emplaced every 56 years on average, twice as often as in other intervals. This pattern is common (e.g., MacInnes et al. 2016) and can be explained partly because tsunami chronology preceding the catalog tends to underestimate a number of events in cases of doubtful separation of tsunami deposits from each other in the sections, without a historical record to compare. Therefore, in evaluating tsunami frequency in the historical and prehistoric period, we postulate that we lose information for about half of the paleo-events. Because the largest events (such as 1952 and 1737) leave a more distinct and widespread deposit (Pinegina et al. 2003; MacInnes et al. 2010; Pinegina 2014) we would argue that the loss of paleoseismological information for weaker events is more typical, and that the geological traces of the largest tsunamis are typically well preserved.

4.5. Analysis of Tsunami Recurrence Depending on Tsunami Intensity

For tsunami hazard analysis, it is important to know not only general tsunami recurrence, but also the intensity (strength, size) of each individual tsunami, as well as the recurrence of different sizes of tsunamis. These data are necessary for long-term tsunami and earthquake prediction and for mapping

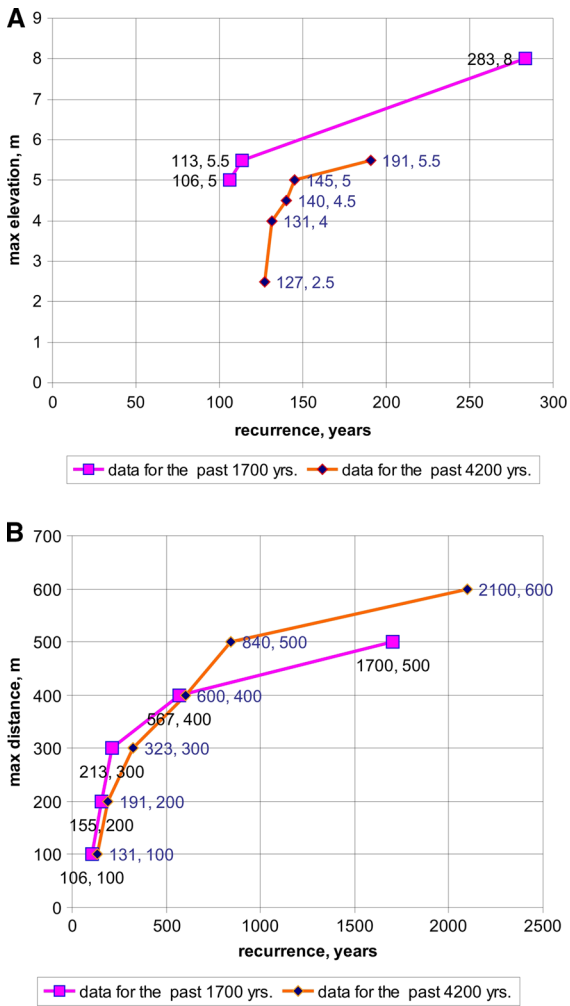


Figure 9

Cumulative graphs of tsunami recurrence for the Avachinsky Bay coast: **a** for exceeded elevations (sediment runup) and **b** for exceeded distances from shoreline (sediment inundation) based on all tsunami deposits present in sections for the past ~ 1700 years (Pinegina 2014) and for the past ~ 4200 years (this study)

tsunami hazard zones and making evacuation plans. We use cumulative graphs of tsunami-deposit runup and inundation distance versus tsunami-deposit recurrence (Fig. 9a, b). To generate higher statistical significance, we have used both newly obtained data and previously published data from 6 (of 9 on Fig. 3) profiles on the Avachinsky Bay coast for the past 1700 years (Pinegina 2014) and from 7 (of 9) profiles with historical events (Pinegina and Bazanova 2016), as well as profiles 1 and 3 (of 9) reported herein, for the past 4200 years.

The runup heights determined from 6 profiles for 1700 years (plus historical cases) are slightly higher than from the two profiles for 4200 years (Fig. 9a), likely because runup heights determined from tsunami deposits always depend on the actual heights existing on a coastal topographic profile. Thus, because profiles 1 and 3 are relatively low, the orange line on Fig. 9a is offset to the right, that is, it shows lower frequencies for tsunamis with runup greater than 5 m, even though in the same bay. Thus, we base our overall analysis on the more complete (though shorter time-scale) dataset (purple line). We conclude that tsunamis with a height of 5 m or more occur on the coast of Avachinsky Bay every 100 (106.5) years on average, while 8 m and higher events occur every 280 (283.6) years on average (purple line in Fig. 9a).

On the other hand, lower profiles permit longer inundation distances, which are shown by the shorter recurrence intervals of inundation of 500 m or more for the orange line in Fig. 9b. The scatter at shorter inundation distances and the differences between the profile sums (purple and orange) is likely not statistically significant. Tsunamis with an inundation distance ≥ 100 m occur every 100 years on average, and tsunamis with inundation ≥ 500 m occur every 840 years on lower profiles and every 1700 years, on average on higher profiles (Fig. 9b).

There is no direct relationship between graphs (a) and (b) in Fig. 9 for a number of reasons, including the coastal topography, as discussed above. Tsunami wavelength (and therefore, inundation) and tsunami height (and therefore, runup) are dependent on earthquake source parameters. Tsunami wavelength and wave period are largely set by source width, whereas initial tsunami height depends on source depth and slip amplitude (Cox and Machemehl 1986).

4.6. Discussion: Seismic Potential of the Kurile-Kamchatka Subduction Zone

Historical earthquakes causing significant tsunamis in Avachinsky Bay have included $M_w > 8$ events from the southern part of Kronotsky Bay (1923) to south Kamchatka (1737 and 1952) (Figs. 1, 3; Pinegina and Bazanova 2016). Inundation

distances for all historical tsunamis on 9 topographic profiles varied from 180 to 480 m, and runup heights from 3.5 to 6.3 m. Along the northern coast of Avachinsky Bay tsunami intensity of the 1952 and 1737 mega-events ($M_w \sim 9$) was similar to the still-large but smaller events with magnitudes 8–8.5. Based on tsunami deposits preserved on the Avachinsky Bay coast, analysis of paleotsunami intensity over the past ~ 4200 years shows that prehistoric events were quite comparable to historical events (Table 2), including the great 1737 and 1952 cases.

In southern Kamchatka (south of Petropavlovsk-Kamchatsky) and the northern Kurile Islands, according to available geological and historical data, the tsunamis of 1737 and 1952 were significantly larger than in Avachinsky Bay, with runup heights of more than 15–20 m and inundation distances of over 1000 m (Krashennikov 1786; Zayakin and Luchina 1987; MacInnes et al. 2010; Pinegina 2014). Moreover, investigations of paleotsunami deposits in this same region show that tsunami intensity (runup and inundation) for some paleo-events is comparable to 1952 and 1737 (Pinegina 2014). These data allow us to conclude that the southern segment of the Kamchatka subduction zone can generate stronger earthquakes and regionally larger tsunamis than from Avachinsky Bay northward, including Kamchatsky Bay (KaB on Fig. 2a; Bourgeois and Pinegina 2018). Avachinsky and Kamchatsky bays also have comparable recurrence intervals for runup and inundation (slightly shorter recurrence for long inundations in Kronotsky). A similar statistical analysis has yet to be applied to south Kamchatka data.

The possible causes of such distribution of seismicity do not yet have an accepted explanation, but the observed differences are almost certainly associated with variations of subduction-zone parameters along Kamchatka. For example, there is an apparent southward increase in coupling between the Pacific and Okhotsk plates along the subduction zone (Bürgmann et al. 2005). Bürgmann et al. (2005) believe that there is a clear correlation between/among currently locked segments of the subduction zone, locations of the strongest historical earthquake sources, positions of negative gravity anomalies, and seafloor relief. Their interpretation of satellite geodetic measurements data (GPS) suggests that in front of

south Kamchatka there is a zone with the most significant plate coupling; therefore, large-scale slip occurs at times in this region, accompanied by earthquakes with $M_w \sim 9$ and their attendant tsunamis.

MacInnes et al. (2010) interpreted the presence of a high-slip region along southern Kamchatka based on modeling multi-segment displacement amplitudes for the source of the 1952 Kamchatka great earthquake and comparing those amplitudes to 1952 tsunami runup from historical records and tsunami-deposit data. They concluded that the tsunami runup was best explained by stronger deformation along south Kamchatka. Paleotsunami intensity along the south Kamchatka coast is also large (Pinegina 2014) and suggests millennial-scale consistency in subduction-zone behavior.

An oceanward shift of the northern edge of the subducted part of Pacific plate, or trench rollback, which begins at about the latitude of Shipunsky Peninsula (Lander and Shapiro 2007) may also explain weaker coupling between the plates along the northern subduction zone. The possibility of the so-called trench rollback has been demonstrated by physical and numerical modeling (Schellart et al. 2007; Stegman et al. 2006). The shift of the eastern part of the Central Kamchatka Depression toward the ocean (Kozhurin et al. 2008; Kozhurin and Zelenin 2017) also supports a hypothesis of slab retreat.

5. Summary and Conclusion

As a result of tephrostratigraphy studies and radiocarbon dating, we have constructed a composite tephrochronological section for the central part of Avachinsky Bay. This section covers the past ~ 4200 years and includes 28 horizons of tephra with determined ages. This combined chronological framework was the basis for reconstructing an age sequence for paleoseismic events imprinted in tsunami deposits. This part of our study has an independent importance as a set of reliable data for various other investigations. For example, our descriptions of sections allow estimating the frequency of tephra falls for volcanic hazard assessment.

Deposits of 33 tsunamis, including 5 of historical age (back to AD 1737), were identified along the Avachinsky Bay coast in excavations going back ~ 4200 years. For each we determined tsunami inundation distance and runup height using corrections for ancient shoreline positions. Runup heights from tsunami deposits are about 2–6 m, with typical inundation 150–450 m; some tsunamis left deposits at distances of more than 500–600 m, probably due to propagation upstream along a river. Clearly variations in these numbers are related not just to tsunami intensity but also to local topography.

The average tsunami recurrence in Avachinsky Bay is 56 years for the historical period (to AD 1737) and ~ 100 –133 years for the past few millennia, showing a direct relationship between recurrence interval (in years) and tsunami size (in m, runup or inundation). From our data we conclude that about half the prehistoric events, mostly weaker ones, are missed in a chronology constructed from tsunami deposits, whereas deposits of the most significant tsunamis are expected to be preserved in the geological record. Obtained data show the important relationship between tsunami recurrence and runup, and tsunami recurrence and inundation. For example, tsunamis with runup ≥ 5 m occur along Avachinsky Bay once in 100 years on average, ≥ 8 m once in 280 years on average. Tsunamis with an inundation of ≥ 100 m occur every 100 years on average, ≥ 500 m every 840 years on average.

We conclude that the decrease in tsunami intensity along the Avachinsky Bay coast in comparison with south Kamchatka can be explained by different parameters of seismicity caused either by variations in plate coupling, or in plate convergence rate, or by both these factors. This conclusion is supported by the long-term consistency of historical and paleo-tsunami data at a given location along the subduction zone, and yet the variability from location to location from Kamchatsky Bay (Bourgeois and Pinegina 2018) to this study site (Avachinsky Bay) to southern Kamchatka (Pinegina 2014).

Judging from our paleoseismic analysis this field area compared to other studies along the subduction zone, the southern part of the Kamchatka subduction zone can generate stronger earthquakes and tsunamis than its northern part. This difference tends toward

agreement of other analyses of the subduction zone but cannot distinguish a specific cause. The obtained data about tsunami history at Avachinsky Bay and other sites along the Kuril-Kamchatka subduction zone are important for the entire Pacific region. According to available data (tsunami catalog for the Hawaiian Islands), we can conclude that tsunamis from Kamchatka earthquakes with $M_w \geq 8.3$ could be hazardous on remote Pacific coasts.

Acknowledgements

This work was supported by Grants from RFBR #15-05-02651, #18-05-00407 and 18-5-003 FEB RAS (to Pinegina). Expeditionary studies partly supported by Grants RFBR #16-05-00090, #15-05-05505, and RNF (project #14-50-00095).

Author contributions All authors participated in field work. TKP is primarily responsible for the tsunami-deposit analyses, radiocarbon calibration and writing the manuscript; LIB is primarily responsible for the tephrostratigraphy and writing the manuscript; EAZ made all geodetic measurements and calculations and helped prepare the manuscript; JB worked with all aspects of the manuscript.

Compliance with ethical standards

Conflict of interest The authors declare they have no conflicts of interest.

REFERENCES

- Abe, T., Goto, K., & Sugawara, D. (2012). Relationship between the maximum extent of tsunami sand and the inundation limit of the 2011 Tohoku-oki tsunami on the Sendai Plain, Japan. *Sedimentary Geology*, 282, 142–150.
- Bazanov, L. I. (2013). 12,000-year of explosive activity at Avachinsky volcano. In *Volcanism and related processes. Abstracts of the regional conference dedicate to Volcanologists Day* (pp. 69–70). IVS FEB RAS, Petropavlovsk-Kamchatsky (in Russian).
- Bazanov, L. I., Braitseva, O. A., Dirksen, O. V., Sulerzhitsky, L. D., & Danhara, T. (2005). Ashfalls from the largest Holocene eruptions along the Ust'-Bol'sheretsk—Petropavlovsk-Kamchatsky traverse: sources, chronology, recurrence. *Journal of Volcanology and Seismology*, 6, 30–46. (in Russian with English abstract).
- Bazanov, L. I., Braitseva, O. A., Melekestsev, I. V. & Puzankov, M. Y. (2001). Potential hazards from the Avachinsky volcano eruptions. In B. V. Ivanov (Ed.), *Geodynamics and volcanism of the Kurile-Kamchatka Island-Arc system* (pp. 390–407) (in Russian with English abstract).

- Bazanova, L. I., Braitseva, O. A., Puzankov, M. Y., & Sulerzhitsky, L. D. (2003). Catastrophic plinian eruptions of the initial cone-building stage of the Young Cone of Avachinsky volcano (Kamchatka). *Vulkanologiya i Seismologiya (Journal of Volcanology and Seismology)*, 5, 20–40. (in Russian with English abstract).
- Bazanova, L. I., Melekestsev, I. V., Ponomareva, V. V., Dirksen, O. V., & Dirksen, V. G. (2016). Late Pleistocene and Holocene volcanic catastrophes in Kamchatka and in the Kurile islands. Part 1. Types and classes of catastrophic eruptions as the leading components of volcanic catastrophism. *Journal of Volcanology and Seismology*, 10(3), 151–169.
- Bourgeois, J. (2009). Geologic effects and records of tsunamis. In Robinson, A.R. & Bernard, E.N., eds., *The Sea*, Vol. 15, Tsunamis. Harvard University Press, p 53–91.
- Bourgeois, J., & Pingina, T. K. (2018). 1997 Kronotsky earthquake and tsunami and their predecessors, Kamchatka, Russia. *Natural Hazards and Earth System Sciences*, 18, 335–350.
- Bourgeois, J., Pingina, T., Ponomareva, V., & Zaretskaia, N. (2006). Holocene tsunamis in the southwestern Bering Sea, Russian Far East, and their tectonic implications. *Geological Society of America Bulletin*, 118(3/4), 449–463.
- Braitseva, O. A., Bazanova, L. I., Melekestsev, I. V., & Sulerzhitsky, L. D. (1998). Largest Holocene eruptions of Avacha volcano, Kamchatka (7250–3700 ¹⁴C years B.P.). *Volcanology and Seismology*, 20(1), 1–27.
- Braitseva, O. A., Ponomareva, V. V., Sulerzhitsky, L. D., Melekestsev, I. V., & Bailey, J. (1997a). Holocene key-marker tephra layers in Kamchatka, Russia. *Quaternary Research*, 47(2), 125–139.
- Braitseva, O. A., Sulerzhitsky, L. D., Ponomareva, V. V., & Melekestsev, I. V. (1997b). Geochronology of the greatest Holocene explosive eruptions in Kamchatka and their imprint on the Greenland glacier shield. *Transactions (Doklady) of the Russian Academy of Sciences. Earth Science Sections*, 352(1), 138–140.
- Bronk, R. C. (2009). Bayesian analysis of radiocarbon dates. *Radiocarbon*, 51(1), 337–360.
- Bürgmann, R., Kogan, M. G., Steblou, G. M., Hilley, G., Levin, V. E. & Apel, E. (2005). Interseismic coupling and asperity distribution along the Kamchatka subduction zone. *Journal of Geophysical Research: Solid Earth*, 110(B7). <https://doi.org/10.1029/2005JB003648>
- Cox, J. C., & Machemehl, J. (1986). Overload bore propagation due to an overtopping wave. *Journal of Waterway, Port, Coastal, and Ocean Engineering*, 112(1), 161–163.
- Dirksen, O. V., & Bazanova, L. I. (2010). An eruption of the veer cone as a volcanic event during the increase of volcanic activity at the beginning of the christian era. *Journal of Volcanology and Seismology*, 4(6), 378–384.
- Goto, K., Chagué-Goff, C., Fujino, S., Goff, J., Jaffe, B., Nishimura, Y., et al. (2011). New insights of tsunami hazard from the 2011 Tohoku-oki event. *Marine Geology*, 290(1), 46–50.
- Gusev, A. A. (2004). The schematic map of the source zones of large Kamchatka earthquakes of the instrumental epoch. In Gordeev E. I., Chebrov V. N. (Eds.), “*Complex seismological and geophysical researches of Kamchatka. To 25th Anniversary of Kamchatkan Experimental and Methodical Seismological Department*” (p. 445), Petropavlovsk-Kamchatsky (in Russian).
- Gusev, A. A. (2006). Large earthquakes in Kamchatka: locations of epicentral zones for the instrumental period. *Journal of Volcanology and Seismology*, 6, 39–42. (in Russian with English abstract).
- Kozhurin, A. I., Ponomareva, V. V., & Pingina, T. K. (2008). Active faulting in the south of Central Kamchatka. *Bulletin of Kamchatka Regional Association “Educational-Scientific Center”*. *Earth Sciences*, 12(2), 10–27. (in Russian with English abstract).
- Kozhurin, A. I., & Zelenin, E. A. (2017). An extending island arc: the case of Kamchatka. *Tectonophysics*, 706, 91–102.
- Krashenninnikov, S.P. (1786). Description of the land of Kamchatka: vol. 1 (p. 438). Imperial Academy of Sciences (in Russian).
- Krashenninnikov, S., Portnyagin, M. & Bazanova, L. (2010). Chemical evolution of Avachinsky volcano (Kamchatka) during the Holocene. Geophysical Research Abstracts. European Geosciences Union 12, EGU2010-633-1.
- Lander, A. V., & Shapiro, M. N. (2007). The Origin of the Modern Kamchatka Subduction Zone. In Eichelberger J. et al., eds., *Volcanism and Subduction: The Kamchatka Region*, 57–64.
- MacInnes, B., Bourgeois, J., Pingina, T. K., & Krchunovskaya, E. A. (2009a). Before and after: geomorphic change from the 15 November 2006 Kuril Island tsunami. *Geology*, 37(11), 995–998.
- MacInnes, B., Krchunovskaya, E., Pingina, T., & Bourgeois, J. (2016). Paleotsunamis from the central Kuril Islands segment of the Japan-Kuril-Kamchatka subduction zone. *Quaternary Research*, 86(1), 54–66.
- MacInnes, B., Pingina, T. K., Bourgeois, J., Razhigaeva, N. G., Kaistrenko, V. M., & Kravchunovskaya, E. A. (2009b). Field survey and geological effects of the 15 November 2006 Kuril tsunami in the Middle Kuril Islands. *Pure and Apply Geophysics*, 166, 9–36.
- MacInnes, B. T., Weiss, R., Bourgeois, J., & Pingina, T. K. (2010). Slip distribution of the 1952 Kamchatka great earthquake based on near-field tsunami deposits and historical records. *Bulletin of the Seismological Society of America*, 100, 1695–1709.
- Melekestsev, I. V., Braitseva, O. A., Bazanova, L. I., Ponomareva, V. V., & Sulerzhitskiy, L. D. (1996). A particular type of catastrophic explosive eruptions with reference to the Holocene subcaldera eruptions at Khangar, Khodutka Maar, and Baraniy Amfiteatr volcanoes in Kamchatka. *Volcanology and Seismology*, 18(2), 135–160.
- Melekestsev, I. V., Braitseva, O. A., Dvigalo, V. N., & Bazanova, L. I. (1994a). Historical eruptions of Avacha volcano, Kamchatka. Attempt of modern interpretation and classification for long-term prediction of the types and parameters of future eruptions. Part 1 (1737–1909). *Volcanology and Seismology*, 15(6), 649–666.
- Melekestsev, I. V., Braitseva, O. A., Dvigalo, V. N., & Bazanova, L. I. (1994b). Historical eruptions of Avacha Volcano, Kamchatka. Attempt of modern interpretation and classification for long-term prediction of the types and parameters of future eruptions. Part 2 (1926–1991). *Volcanology and Seismology*, 16(2), 93–114.
- National Centers for Environmental Information (NCEI, formerly NGDC), Natural Hazards Data, Images and Education, Tsunami and Earthquake databases [online]. <https://www.ngdc.noaa.gov/hazard/hazards.shtml>. Accessed 16 Mar 2018
- Pingina, T. K. (2014). Time-space distribution of tsunamigenic earthquakes along the pacific and bering coasts of Kamchatka: insight from paleotsunami deposits (p. 235). Doctor of

- Geological Science dissertation, Institute of Oceanology RAS, Moscow (**in Russian**).
- Pinegina, T. K., & Bazanova, L. I. (2016). New data on characteristic of historical tsunami on the coast of Avacha Bay (Kamchatka). *Bulletin of Kamchatka Regional Association "Educational-scientific center"*. *Earth Sciences*, 31(3), 5–17. (**in Russian with English abstract**).
- Pinegina, T. K., Bazanova, L. I., Melekestsev, I. V., Braitseva, O. A., Storcheus, A. V., & Gusyakov, V. K. (2000). Prehistorical tsunamis in Kronotskii Gulf, Kamchatka, Russia: a progress report. *Volcanology and Seismology*, 22(2), 213–226.
- Pinegina, T. K., Bazanova, L. I., Zelenin, E. A. & Kozhurin, A. I. (2015). Identification of Holocene mega-earthquakes along the Kurile-Kamchatka subduction zone. In Chebrov, V. N. (Ed.), *Proceedings of 5th science and technology conference "Problems of complex geophysical monitoring of the Russian Far East"* (pp. 373–377), Petropavlovsk-Kamchatsky, Sept. 27–Oct. 3. Obninsk: GS RAS (**in Russian**).
- Pinegina, T. K., Bourgeois, J., Bazanova, L. I., Braitseva, O. A. & Egorov, Y. O. (2002). Tsunami and analysis of tsunami risk at Khalatyryka beach region of Petropavlovsk-Kamchatsky, pacific coast of Kamchatka. In *Proceedings of the International workshop "Local tsunami warning and mitigation"* (pp. 122–131), Petropavlovsk-Kamchatsky, September 10–15, Moscow, Yanus-K.
- Pinegina, T. K., Bourgeois, J., Bazanova, L. I., Melekestsev, I. V., & Braitseva, O. A. (2003). Millennial—scale record of Holocene tsunamis on the Kronotskiy Bay coast, Kamchatka, Russia. *Quaternary Research*, 59, 36–47.
- Pinegina, T. K., Bourgeois, J., Kravchunovskaya, E. A., Lander, A. V., Arcos, M. E. M., Pedoja, K., et al. (2013). A nexus of plate interaction: segmented vertical movement of Kamchatsky Peninsula (Kamchatka) based on Holocene aggradational marine terraces. *The Geological Society of America Bulletin*, 125(9/10), 1554–1568.
- Reimer, P. J., Bard, E., Bayliss, A., Beck, J. W., Blackwell, P. G., Bronk, R. C., et al. (2013). IntCal13 and Marine13 Radiocarbon age calibration Curves 0–50,000 years cal BP. *Radiocarbon*, 55(4), 1869–1888.
- Schellart, W. P., Freeman, J., Stegman, D. R., Moresi, L., & May, D. (2007). Evolution and diversity of subduction zones controlled by slab width. *Nature*, 446, 308–311.
- Soloviev, S. L. (1972). Recurrence of earthquakes and tsunamis in the Pacific Ocean. In *Proceedings of SakhKNII*, 29. *The waves of the tsunami* (pp. 7–47). Yuzhno-Sakhalinsk (**in Russian**).
- Soloviev, S. L. (1978). Basic data on the tsunami on the Pacific coast of the USSR, 1737-1976. In Nayka, M. (Ed.), *The study of tsunamis in the open ocean* (pp. 61–136) (**in Russian**).
- Soloviev, S. L. & Ferchev, M. D. (1961). A summary of data on the tsunami in the USSR. In *Bull. Council on Seismology*, 9 (pp. 23–55). USSR Academy of Sciences (**in Russian**).
- Stegman, D. R., Freeman, J., Schellart, W. P., Moresi, L., & May, D. (2006). Influence of trench width on subduction hinge retreat rates in 3-D models of slab rollback. *Geochemistry Geophysics Geosystems*, 7(3), 1–22.
- Woodroff, S. A., & Horton, B. P. (2005). Holocene sea-level changes in the Indo-Pacific. *Journal of Asian Earth Sciences*, 25(1), 29–43.
- Zayakin, Y. A. & Luchinina, A. A. (1987). Catalogue tsunamis on Kamchatka. In (p. 51). Obninsk: Vniigmi-Mtsd (**Booklet in Russian**).

(Received February 21, 2018, revised March 7, 2018, accepted March 8, 2018)